

Hot Electrons in Microscale Thin-Film Schottky Barriers for Enhancing Near-Infrared Detection

Ahmad I. Nusir, *Student Member, IEEE*, Grant P. Abbey, Avery M. Hill, Omar Manasreh, *Senior Member, IEEE*, and Joseph B. Herzog

Abstract—Metallic microstructures composed from Au thin films were designed and fabricated to enhance the near-infrared detection of photodetectors based on GaAs. The devices showed significant increase in the photocurrent and the spectral response due to the generation of hot electrons in the Au thin films and their injection into the semiconductor. Enhancement in the order of 120% was achieved in the photocurrent after applying an array of Au thin films with a thickness of 10 nm. Furthermore, a photocurrent-sweep using red laser showed an increase in the photocurrent of the device, as the laser was swept over the Au thin film. The effect of adding Ti adhesive layer on damping the photocurrent enhancement was further studied by varying the thickness of Ti between 0 and 4 nm.

Index Terms—Hot electrons, photodetectors, near-infrared, thin-film.

I. INTRODUCTION

METALLIC structures with various dimensions and shapes have been utilized either as contacts or to enhance the response of different optoelectronics devices such as solar cells, light emitting diodes, and photodetectors [1]–[3]. Metal has a large density of free carriers that can be excited by photo-absorption creating energetic carriers, known as hot electrons [4], [5]. Devices based on hot electrons are fabricated by depositing metal on the surface of semiconductor forming a Schottky junction [6], [7]. The barrier height of the Schottky junction depends on the difference between the work function of the metal and the electron affinity of the semiconductor [8]. Hot electrons with sufficient energy are injected through the metal-semiconductor interface into the conduction band of the semiconductor and collected as a photocurrent [9], [10]. In this case, additional spectral tuning could be achieved through collecting photons with energy lower than the bandgap of the semiconductor [11], [12]. Different Schottky barriers were

used to inject hot electrons into bulk semiconductor such as Si and TiO₂ and two-dimensional materials: graphene and MoS₂ [13]–[16].

Photodetectors based on hot electrons have been demonstrated by using variety of nanometer-scale metallic structures and optical nanoantennas [17], [18]. The devices showed improvement in the performance due to the generation of hot electrons by surface plasmon decay [19]–[21]. However, the plasmonic structures are in nanoscale, which are challenging to fabricate requiring expensive patterning methods such as electron-beam (e-beam) lithography or focused ion beam milling [22], [23]. Fabricating microscale metallic structures that could still generate hot electrons will gain the merits of using cost-effective techniques like standard optical photolithography making it compatible for mass production. For these devices, metals like Au or Ag are used due to the large free-carrier concentration. Additionally, an adhesive layer of Ti or Cr is necessary to ensure stability of the metal during the lift-off process [24]. In this letter, we report on the fabrication and characterization of microscale Au thin-films that are designed to enhance the photoresponsivity of near-infrared photodetector based on GaAs. Enhancement in both the current-voltage characteristics and the spectral response was achieved after applying the microscale array with various Au thin-films thickness. Photocurrent-sweep showed significant increase in the photocurrent as the laser was swept over the Au thin-films due to the generation of hot electrons in Au and the subsequent injection into the semiconductor. Furthermore, the effect of adding Ti adhesive layer on the photocurrent enhancement was studied as function of different Ti thickness.

II. EXPERIMENTAL METHODS

The array consists of pairs of microscale pads ($20 \times 20 \mu\text{m}$) spaced by $2 \mu\text{m}$) as shown in Fig. 1 (a). The pads are made from Au thin-films with thickness ranging from 10 to 50 nm. The near-infrared photodetector consists of three planar Au electrodes deposited on a semi-insulating GaAs substrate, as shown in Fig. 1 (b). The separation between the electrodes is 0.95 mm and the Au thickness in each electrode is 50 nm. Each electrode has a width and a length of $50 \mu\text{m}$ and 1.75 mm, respectively. Wire bonds were connected to the outer electrode frame and the middle electrode to enable measuring the photocurrent under different biasing conditions. The middle electrode was designed with a triangular shape at

Manuscript received May 16, 2016; revised June 12, 2016; accepted July 11, 2016. Date of publication July 13, 2016; date of current version September 13, 2016. This work was supported in part by the National Aeronautics and Space Administration–EPSCoR under Grant 242026-1BBX11AQ36A and in part by the National Science Foundation under Grant 1359306.

A. I. Nusir and O. Manasreh are with the Department of Electrical Engineering, University of Arkansas, Fayetteville, AR 72701 USA (e-mail: ainusir@uark.edu; manasreh@uark.edu).

G. P. Abbey is with the Department of Electrical Engineering and Computer Science, Mississippi State University, Mississippi State, MS 39762 USA (e-mail: grantpabbey@gmail.com).

A. M. Hill and J. B. Herzog are with the Department of Physics, University of Arkansas, Fayetteville, AR 72701 USA (e-mail: amh029@uark.edu; jberzog@uark.edu).

Color versions of one or more of the figures in this letter are available online at <http://ieeexplore.ieee.org>.

Digital Object Identifier 10.1109/LPT.2016.2591261

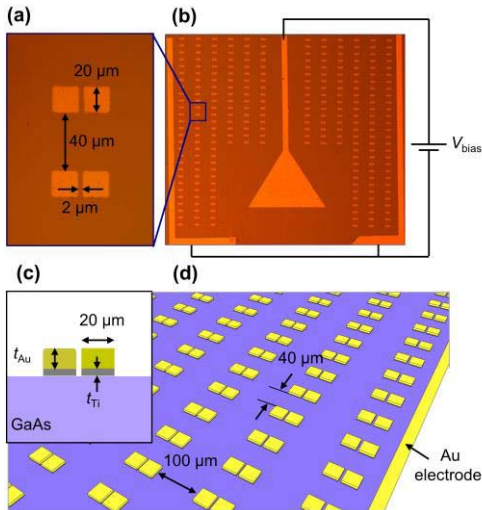


Fig. 1. (a) Microscopic image showing pair of $20 \times 20 \mu\text{m}$ pads spaced by $2 \mu\text{m}$. (b) Top view of the photodetector with the microstructure array. (c) Cross-section view of pads made from thin-films of Au with thickness of t_{Au} and Ti with thickness of t_{Ti} deposited on GaAs. (d) Schematic showing the microstructure array deposited between the photodetector electrodes.

the top for wire-bonding. When the device is biased, electric field points from the middle electrodes to the two outermost electrodes. The semi-insulating GaAs substrate has a resistivity of $2.2 \times 10^8 \Omega \cdot \text{cm}$ and carrier concentration of $5 \times 10^6 \text{ cm}^{-3}$.

The fabrication of the microstructure array and the photodetector electrodes was prepared using standard optical photolithography, metal evaporation, and lift-off inside class-100 clean room. The deposition of the metals was performed using Angstrom Nexdep e-beam evaporator at pressure of 1.5×10^{-7} torr, and the lift-off was prepared using PRS-1000 photoresist stripper purchased from J. T Baker. The cross section of the pads made from Au thin-films is illustrated in Fig. 1 (c) and shows a Ti adhesive layer, with thickness of t_{Ti} , followed by an Au top layer with thickness of t_{Au} . The row and column spacing between the pair of pads were designed to be 40 and $100 \mu\text{m}$, respectively, as shown in Fig. 1 (d). With these dimensions, the microstructure array will cover 4% of the total area between the electrodes.

The photodetectors were characterized before and after adding the Au microstructure array by measuring the photocurrent-voltage ($I_{\text{photo}}-V$) characteristics and the spectral response. The $I_{\text{photo}}-V$ characteristics were extracted using a Keithley 4200 semiconductor parameter analyzer under the illumination of a broadband light source that covers the spectral range from 360 to 1800 nm with a power of 7 mW . A linear photocurrent sweep was measured for the devices at a bias voltage of 5 V and under the excitation of a red laser (632 nm) with a power of $400 \mu\text{W}$. The laser was focused using a $50\times$ objective with numerical aperture of 0.55 . The spectral response measurements of the devices were performed using a Bruker IFS 125HR Fourier transform (FT) spectrometer with a quartz beam-splitter.

III. RESULTS AND DISCUSSION

The $I_{\text{photo}}-V$ characteristics were measured before ($I_{w/o}$) and after (I_w) depositing the Au microstructure array onto the

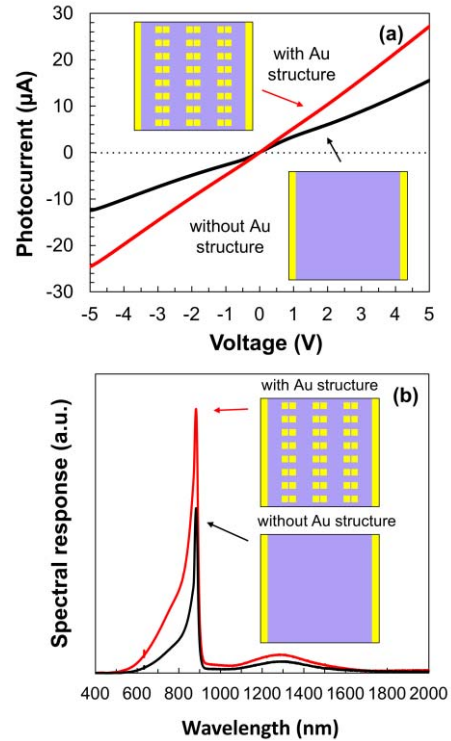


Fig. 2. (a) $I_{\text{photo}} - V$ curve and (b) spectral response at 5 V bias for device before and after applying array of microscale pads with $t_{\text{Au}} = 50 \text{ nm}$.

device; results are plotted in Fig. 2 (a). In this figure, the array consisted of an Au layer with thickness of $t_{\text{Au}} = 50 \text{ nm}$ and no Ti adhesive layer. Upon adding the microstructure array, the photocurrent at 5 V increases from $12.45 \mu\text{A}$ to $24.5 \mu\text{A}$. This corresponds to an enhancement of 97% in the photocurrent. The enhancement in the photocurrent was calculated using: $\text{Enhancement}(\%) = (I_w - I_{w/o})/I_{w/o}$.

The same device was characterized by measuring the spectral response in the visible and near-infrared regions with and without the Au microstructure array at a bias voltage of 5 V . The spectral response results are plotted in Fig. 2 (b). Enhancement covering the near-infrared spectral regions was observed upon adding the Au microstructure array. The peak in the spectral response located at 1280 nm (0.97 eV), which is below the bandgap of GaAs (1.42 eV), is attributed to the internal photoemission of carriers above the Schottky barrier formed at the Au/GaAs interface. Before adding the microscale array, the internal photoemission occurs across the Schottky barrier between the Au electrode and GaAs. The increase in the spectral response in the wavelength region below 870 nm (1.42 eV) is due to the excitation of carriers in the bulk GaAs. While the rapid decay in the spectral response in the lower wavelength region is due to the response of the quartz beam-splitter in the FT spectrometer. The results in Figs. 2 (a) and (b) were measured with a light source illuminating the entire area of the device.

The dependence of the photocurrent enhancement on the thickness of the thin-films was further investigated. Multiple photodetectors were fabricated with the same electrodes as shown in Fig. 1, and each of these devices was characterized. Then the microstructures composed of Au and Ti thin-films

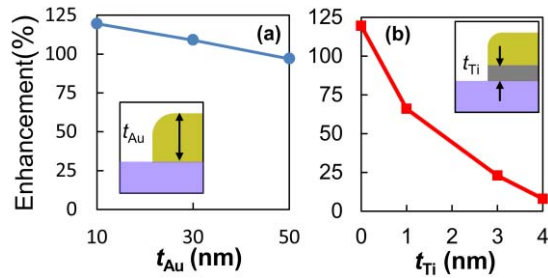


Fig. 3. Enhancement(%) in the photocurrent after applying arrays of: (a) variable Au thickness, and (b) variable Ti thickness.

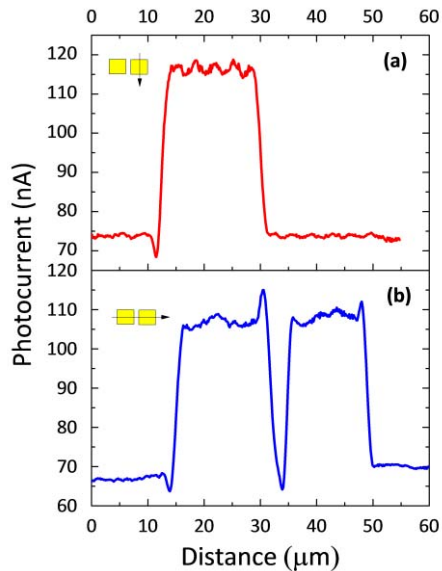


Fig. 4. Photocurrent sweep using red laser across a pair of pads having Au thin-film with thickness of 30 nm for (a) vertical and (b) horizontal scans.

with various thicknesses were added to each of these photodetectors. The enhancement in the photocurrent was found by measuring the $I_{\text{photo}}-V$ curves before and after applying the array of the microscale pads. Figure 3 (a) shows the enhancement in the photocurrent at bias voltage of 5 V as function of Au thickness, $t_{Au} = 10, 30,$ and 50 nm, with no Ti layer ($t_{Ti} = 0$). The enhancement in the photocurrent was reduced from 120% to 97%, as t_{Au} increases from 10 to 50 nm. Next, the photocurrent enhancement was investigated for devices with various thickness of the Ti adhesion layer between the Au and the GaAs, which was varied between 0 to 4 nm. For these measurements, the thickness of the top Au layer was held constant at $t_{Au} = 10$ nm. The results are plotted in Fig. 3 (b), and shows that the photocurrent enhancement was reduced from 120% to 8% as t_{Ti} increased to 4 nm.

A photocurrent sweep was measured for a photodetector with an array of microscale pads ($t_{Au} = 30$ nm and $t_{Ti} = 0$). In this measurement, the focused red laser was linearly swept over a pair of microscale pads vertically and horizontally while the photocurrent between the electrodes was measured and plotted as function of laser position in Figs. 4 (a) and (b), respectively. The photodetector was biased at 5 V during the measurements. In the vertical scan plotted in Fig. 4 (a), the photocurrent off the metallic pads was limited to 74 nA,

and once the laser was swept over the pads the photocurrent increased to 118 nA due to the excitation and injection of hot electrons. The photocurrent sweep of the horizontal scan is shown in Fig. 4 (b). The Au microstructures are considered as source of electrons confined by the Schottky barrier between Au and GaAs. When the red laser with energy of 1.96 eV irradiates the Au microstructures, hot electrons are generated and injected across the Schottky barrier with energy of 0.97 eV. The hot electrons injected into the GaAs will drift under the influence of electric field applied between the electrodes and contribute in enhancing the overall photocurrent. The Au microstructures in this work are floating unlike other designs [4], [13], [25], but due to the high conductivity of Au, it is likely that some current flows through the metal pads.

The result in Fig. 3 (a) shows that the enhancement in the photocurrent depends on thickness of the Au thin-films, as the Au thickness decreases the photocurrent enhancement increases. This result coincide with the theoretical and experimental work reported by Scales *et al.*, and both showed significant increase in the response of the devices using thinner Au films due to the increase in the emission probability of hot electrons into the semiconductor [26]. Very thin Au films can be used to enhance the internal photoemission due to the multiple reflections of hot electrons off the Au/GaAs and Au/air interfaces, and providing more opportunity for electrons emission over the Schottky barrier into the semiconductor [26]. On the other hand, the result in Fig. 3 (b) suggests that the addition of Ti layer between the Au and GaAs will result in decreasing the photocurrent enhancement. As the Ti layer increases the path traveled by the hot electrons from the Au to the GaAs also increases; therefore, the emission probability of electrons reduces [26]. A larger thickness of Ti will increase the distance needed by hot electrons to travel before injected into GaAs and providing more chance for them to lose their energy in collisions and not contribute to the photocurrent [20].

The role of surface plasmon in inducing the generation of hot electrons is small since the plasmons generated at the edge of the structure would quickly decay before they reach the center of the microstructure. Additionally, the photocurrent of the devices did not show dependence on the polarization direction of the incident light, which is typical for plasmonic devices [27]. Yet the microscale array was able to show significant increase in the photocurrent, due to having an array of large Au microstructures. Since the microstructures have a much larger area than nanoscale plasmonic structures, they can absorb more light, which therefore generates many hot electrons. The photocurrent enhancement in this work reached values of 120%, which is higher as compared to the reported enhancement achieved using plasmonic nanoparticles for solar cells, which was limited to 58% [28].

IV. CONCLUSION

In summary, this work demonstrates the utilization of hot electrons generated in Au thin-films with microscale dimensions to enhance the photoresponsivity of near-infrared photodetectors. The microstructure array of Au thin-films showed increase in the photocurrent as the Au thickness reduces, due to the increase in the emission probability of hot electrons

over the Au/GaAs interface. Moreover, the spectral response exhibited enhancement at a wavelength of 1280 nm caused by the internal photoemission of hot electrons. The enhancement was also recorded by measuring the photocurrent sweep. The thin-film microscale array proved that significant enhancement could be achieved using hot electrons while still gaining the merits of using photolithography, a cost-effective fabrication technique. This work has determined important design considerations for future devices based on hot electrons.

REFERENCES

- [1] V. E. Ferry *et al.*, "Light trapping in ultrathin plasmonic solar cells," *Opt. Exp.*, vol. 18, no. S2, pp. A237–A245, Jun. 2010, doi: 10.1364/OE.18.00A237.
- [2] R. Koester *et al.*, "High-speed GaN/GaInN nanowire array light-emitting diode on silicon(111)," *Nano Lett.*, vol. 15, no. 4, pp. 2318–2323, Apr. 2015, doi: 10.1021/nl504447j.
- [3] A. I. Nusr and M. O. Manasreh, "Self-powered near-infrared photodetector based on asymmetrical Schottky interdigital contacts," *IEEE Electron Device Lett.*, vol. 36, no. 11, pp. 1172–1175, Nov. 2015, doi: 10.1109/LED.2015.2478395.
- [4] A. Sobhani *et al.*, "Narrowband photodetection in the near-infrared with a plasmon-induced hot electron device," *Nature Commun.*, vol. 4, p. 1643, Mar. 2013, doi: 10.1038/ncomms2642.
- [5] Y. K. Lee, C. H. Jung, J. Park, H. Seo, G. A. Somorjai, and J. Y. Park, "Surface plasmon-driven hot electron flow probed with metal-semiconductor nanodiodes," *Nano Lett.*, vol. 11, no. 10, pp. 4251–4255, Oct. 2011, doi: 10.1021/nl2022459.
- [6] I. Goykhman, B. Desiatov, J. Khurgin, J. Shappir, and U. Levy, "Locally oxidized silicon surface-plasmon Schottky detector for telecom regime," *Nano Lett.*, vol. 11, no. 6, pp. 2219–2224, Jun. 2011, doi: 10.1021/nl200187v.
- [7] C. Scales, I. Breukelaar, and P. Berini, "Surface-plasmon Schottky contact detector based on a symmetric metal stripe in silicon," *Opt. Lett.*, vol. 35, no. 4, pp. 529–531, Feb. 2010, doi: 10.1364/OL.35.000529.
- [8] D. W. Peters, "An infrared detector utilizing internal photoemission," *Proc. IEEE*, vol. 55, no. 5, pp. 704–705, May 1967, doi: 10.1109/PROC.1967.5648.
- [9] W. Wang, A. Klots, D. Prasai, Y. Yang, K. I. Bolotin, and J. Valentine, "Hot electron-based near-infrared photodetection using bilayer MoS₂," *Nano Lett.*, vol. 15, no. 11, pp. 7440–7444, Nov. 2015, doi: 10.1021/acs.nanolett.5b02866.
- [10] A. O. Govorov, H. Zhang, and Y. K. Gun'ko, "Theory of photoinjection of hot plasmonic carriers from metal nanostructures into semiconductors and surface molecules," *J. Phys. Chem. C*, vol. 117, no. 32, pp. 16616–16631, Aug. 2013, doi: 10.1021/jp405430m.
- [11] B. Y. Zheng, Y. Wang, P. Nordlander, and N. J. Halas, "Color-selective and CMOS-compatible photodetection based on aluminum plasmonics," *Adv. Mater.*, vol. 26, no. 36, pp. 6318–6323, Aug. 2014, doi: 10.1002/adma.201401168.
- [12] W. Li and J. Valentine, "Metamaterial perfect absorber based hot electron photodetection," *Nano Lett.*, vol. 14, no. 6, pp. 3510–3514, Jun. 2014, doi: 10.1021/nl501090w.
- [13] M. W. Knight, H. Sobhani, P. Nordlander, and N. J. Halas, "Photodetection with active optical antennas," *Science*, vol. 332, no. 6030, pp. 702–704, 2011, doi: 10.1126/science.1203056.
- [14] C. Clavero, "Plasmon-induced hot-electron generation at nanoparticle/metal-oxide interfaces for photovoltaic and photocatalytic devices," *Nature Photon.*, vol. 8, no. 2, pp. 95–103, Jan. 2014, doi: 10.1038/nphoton.2013.238.
- [15] Z. Fang *et al.*, "Plasmon-induced doping of graphene," *ACS Nano*, vol. 6, no. 11, pp. 10222–10228, Nov. 2012, doi: 10.1021/nn304028b.
- [16] T. Hong, B. Chamlagain, S. Hu, S. M. Weiss, Z. Zhou, and Y.-Q. Xu, "Plasmonic hot electron induced photocurrent response at MoS₂-metal junctions," *ACS Nano*, vol. 9, no. 5, pp. 5357–5363, May 2015, doi: 10.1021/acsnano.5b01065.
- [17] L. Tang *et al.*, "Nanometre-scale germanium photodetector enhanced by a near-infrared dipole antenna," *Nature Photon.*, vol. 2, no. 4, pp. 226–229, Mar. 2008, doi: 10.1038/nphoton.2008.30.
- [18] P. Fan, K. C. Y. Huang, L. Cao, and M. L. Brongersma, "Redesigning photodetector electrodes as an optical antenna," *Nano Lett.*, vol. 13, no. 2, pp. 392–396, Feb. 2013, doi: 10.1021/nl303535s.
- [19] F. W. Carter, D. F. Santavica, and D. E. Prober, "A plasmonic antenna-coupled superconducting near-IR photon detector," *Opt. Exp.*, vol. 22, no. 18, pp. 22062–22071, Sep. 2014, doi: 10.1364/OE.22.022062.
- [20] H. Chalabi, D. Schoen, and M. L. Brongersma, "Hot-electron photodetection with a plasmonic nanostripe antenna," *Nano Lett.*, vol. 14, no. 3, pp. 1374–1380, Mar. 2014, doi: 10.1021/nl4044373.
- [21] M. W. Knight *et al.*, "Embedding plasmonic nanostructure diodes enhances hot electron emission," *Nano Lett.*, vol. 13, no. 4, pp. 1687–1692, Apr. 2013, doi: 10.1021/nl400196z.
- [22] P. Biagioni, J.-S. Huang, and B. Hecht, "Nanoantennas for visible and infrared radiation," *Rep. Prog. Phys.*, vol. 75, no. 2, p. 024402, Jan. 2012, doi: 10.1088/0034-4885/75/2/024402.
- [23] Y. Chen, J. Chen, X. Xu, and J. Chu, "Fabrication of bowtie aperture antennas for producing sub-20 nm optical spots," *Opt. Exp.*, vol. 23, no. 7, pp. 9093–9099, Apr. 2015, doi: 10.1364/oe.23.009093.
- [24] T. G. Habteyes *et al.*, "Metallic adhesion layer induced plasmon damping and molecular linker as a nondamping alternative," *ACS Nano*, vol. 6, no. 6, pp. 5702–5709, Jun. 2012, doi: 10.1021/nn301885u.
- [25] W. Li, Z. J. Coppens, L. V. Besteiro, W. Wang, A. O. Govorov, and J. Valentine, "Circularly polarized light detection with hot electrons in chiral plasmonic metamaterials," *Nature Commun.*, vol. 6, p. 8379, Sep. 2015, doi: 10.1038/ncomms9379.
- [26] C. Scales and P. Berini, "Thin-film Schottky barrier photodetector models," *IEEE J. Quantum Electron.*, vol. 46, no. 5, pp. 633–643, May 2010, doi: 10.1109/JQE.2010.2046720.
- [27] J. B. Herzog, M. W. Knight, Y. Li, K. M. Evans, N. J. Halas, and D. Natelson, "Dark plasmons in hot spot generation and polarization in interelectrode nanoscale junctions," *Nano Lett.*, vol. 13, no. 3, pp. 1359–1364, Mar. 2013, doi: 10.1021/nl400363d.
- [28] E. S. Arinze, B. Qiu, G. Nyirjesy, and S. M. Thon, "Plasmonic nanoparticle enhancement of solution-processed solar cells: Practical limits and opportunities," *ACS Photon.*, vol. 3, no. 2, pp. 158–173, Feb. 2016, doi: 10.1021/acsp Photonics.5b00428.